

Supplementary Information: Unraveling the Mystery of “Tech Red” – a Volatile Technetium Oxide

Keith V. Lawler,^{1,2,*} Bradley C. Childs,¹ Kenneth R. Czerwinski,¹ Alfred P. Sattelberger,^{1,3} Frederic Poineau,¹ and Paul M. Forster,^{1,2,*}

¹Department of Chemistry and Biochemistry, University of Nevada Las Vegas, Las Vegas, NV 89154, USA.

²High Pressure Science and Engineering Center, University of Nevada Las Vegas, Las Vegas, NV 89154, USA.

³Chemical Sciences and Engineering Division, Argonne National Laboratory, Lemont, IL 60439, USA.

Single Molecule Simulation Methods

Simulations were performed with the Q-Chem 4.0 package¹ using the spin-unrestricted generalized gradient approximation (GGA) functional of Perdew, Burke, and Ernzerhof (PBE)² with Grimme’s -D3³ semi-empirical dispersion correction. The simulations employed the def2-TZVP triple- ζ valence with polarization basis set that uses a small core effective core potential (ECP) to describe the Tc core ([Ar]+3d¹⁰) electrons.^{4,5} The ECP was parameterized to account for scalar relativistic effects. The exchange-correlation functional was evaluated on an Euler-Maclaurin-Lebedev quadrature grid with 75 angular points and 302 radial points per atom. All simulations were performed without consideration for molecular or electronic symmetry. All initial guesses were open shell with broken spin symmetry to avoid trapping the solution in a closed-shell saddle point. The energy convergence tolerance was 10⁻⁹ E_h (Hartree) with an integral cutoff of 10⁻¹⁴ E_h. Structures were optimized with the convergence criterion of a maximum gradient component of 10⁻⁴ E_h/Å and a maximum atomic displacement of 3x10⁻⁴ Å. Vibrational frequencies were evaluated by numeric second derivatives using the analytic gradient. Zero point vibrational energies determined from frequency analysis were included to compare the relative energetics. Previously, we demonstrated that PBE-D3³ is very predictive for the structure of Tc₂O₇,^{6,7} however pure GGAs are known to produce several spurious TD-DFT charge transfer states and produce larger errors for the excitation energies of non-local charge transfer excited states.^{8,9} The inclusion

of exact exchange via a long-range correction has been shown to remedy this problem,¹⁰ and for that reason the excitation energies are computed here with TD-DFT using long-range corrected PBE (LRC- ω PBE) with $\omega = 0.3a_0$.^{8,11}

Relative Stabilities, Bonding, and Comparative TD-DFT Spectra

Table S1: Relative stabilities as heat of formation per atom (kcal/mol) compared to an isolated Tc atom, O₂ molecule, and H₂ molecule for each of the lowest energy structures of each stoichiometry and motif. The spin multiplicity of the lowest energy solution is indicated in parentheses.

	0-br	1-br	2-br	3-br
Tc₂O₄	-64.16 (triplet)	-64.11 (singlet)	-65.98 (singlet)	-58.19 (singlet)
Tc₂O₅	-63.32 (triplet)	-66.79 (triplet)	-66.74 (triplet)	-61.30 (singlet)
Tc₂O₆	-65.18 (singlet)	-64.62 (triplet)	-68.29 (singlet)	-

HTcO ₄	Tc ₂ O ₇	TcO ₂	TcO ₃
-53.15 (singlet)	-65.73 (singlet)	-51.45 (quartet)	-58.53 (doublet)

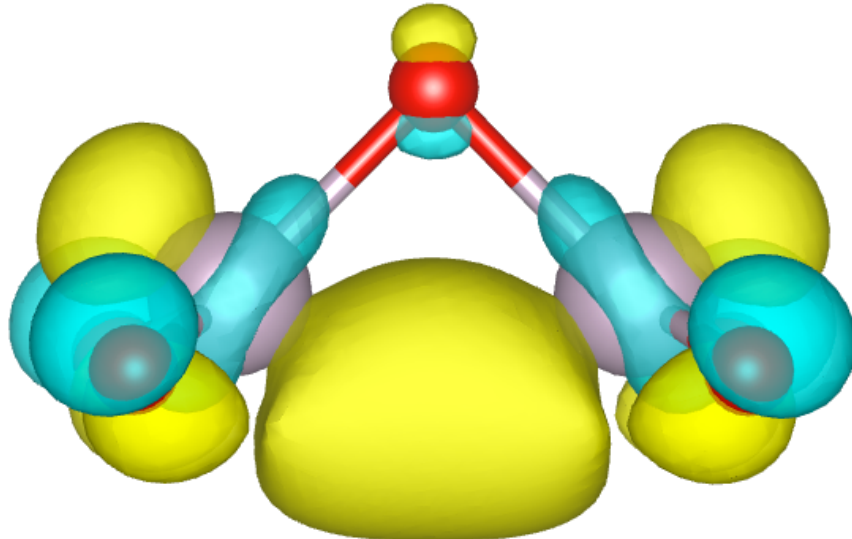


Figure S1: Example of a Tc-Tc σ bonding orbital

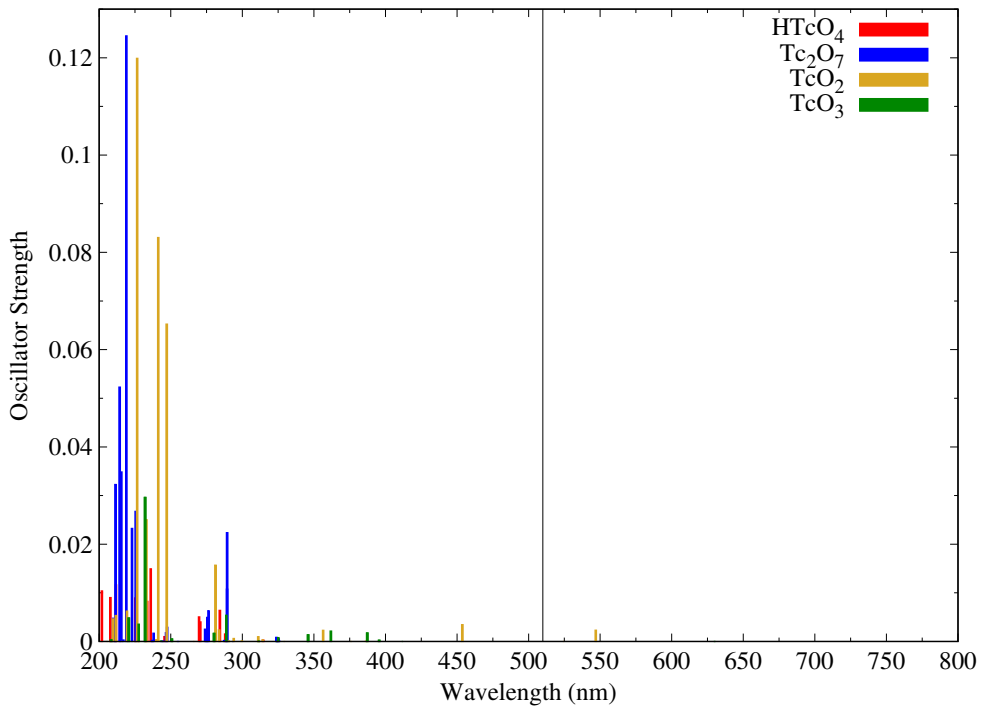


Figure S2: TD-DFT predicted adsorptions for HTcO₄, Tc₂O₇, TcO₃, and TcO₂. A thin line denoting 510 nm has been overlaid.

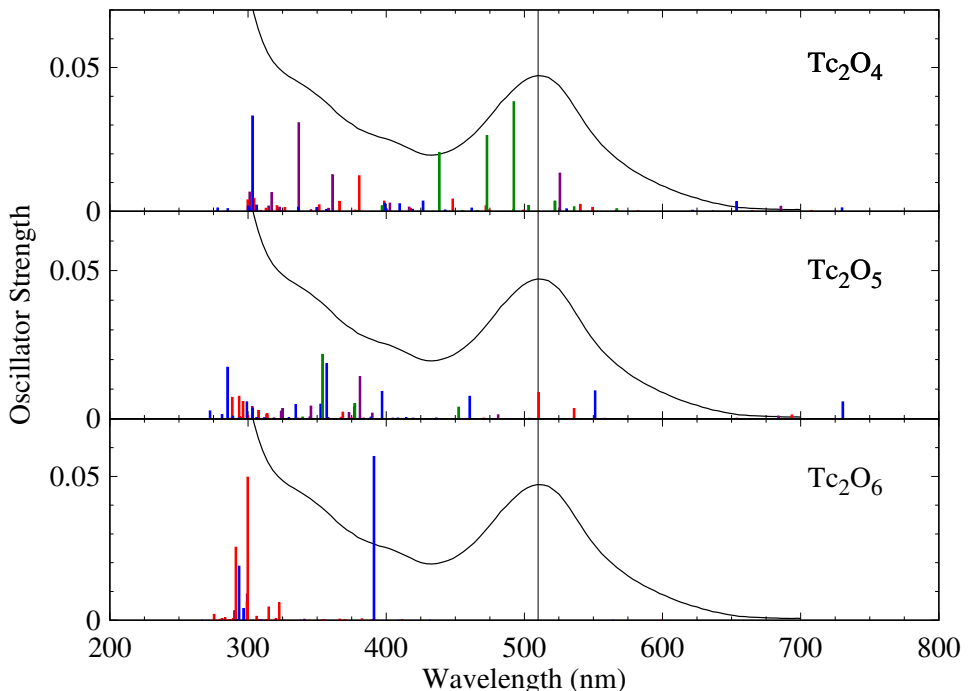


Figure S3: TD-DFT predicted absorption excitations for the species in Figure 1: purple – 0-br, red – 1-br, blue – 2-br, green – 3-br. The experimental curve (scaled by $\frac{1}{4}$) for the red product is overlaid along with a thin line denoting 510 nm.¹²

The triplet state of 1-br Tc₂O₅ is the most stable state of Tc₂O₅, however a singlet state of the molecule was also simulated. The singlet and triplet spin solutions of 1-br Tc₂O₅ differ by only 0.17 kcal/mol (triplet is lower) and have similar electronic and molecular structures: a Tc-Tc bond (see Figure S1), an unpaired *d* electron per Tc, and a Tc-Tc distance of 2.61 and 2.65 Å for the singlet and triplet, respectively. They also have similar predicted spectra, except the target feature is shifted down to 484 nm for the singlet and is a quarter as intense, which confirms that the triplet state is the more likely candidate of the two. Several other functionals were evaluated to test the accuracy of the predicted spectra for 1-br Tc₂O₅, as may be seen in Figure S4.^{2,8,11,13–15} Each of the functionals predicts a similar spectrum, albeit shifted by at most 0.15 eV, which is a reasonable value for the expected error for predicting *d*→*d* transitions in transition metal compounds.¹⁶ Therefore, we will use ±0.15 eV as a reasonable confidence interval for the predicted spectra in this work.

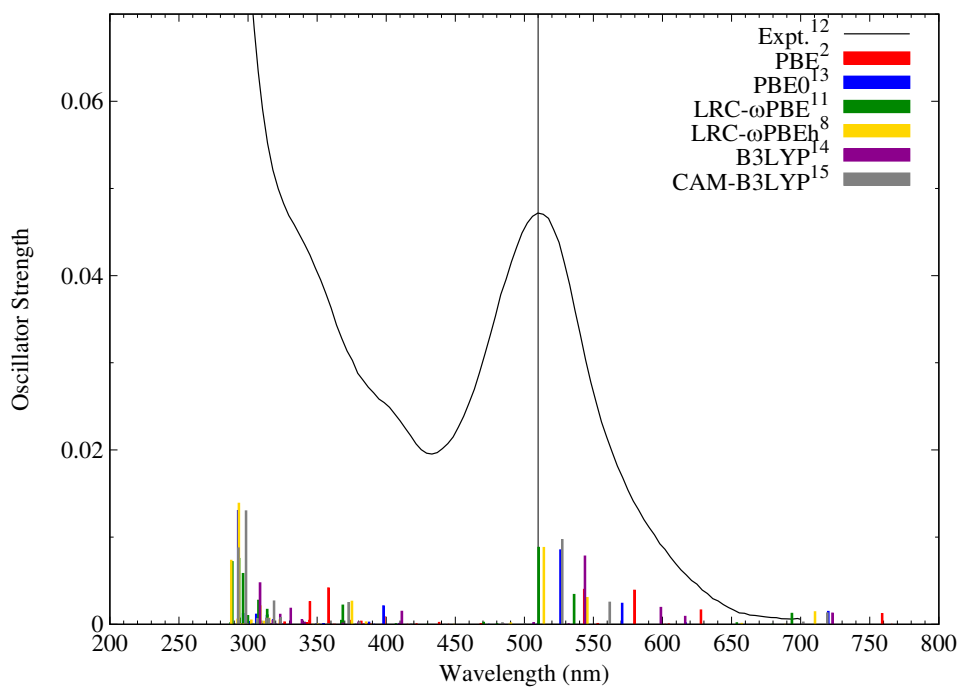


Figure S4: The TD-DFT UV-Vis absorption spectra of 1-br Tc₂O₅ evaluated with several functionals. The experimental curve (scaled by 1/4) for the red product is overlaid along with a thin line denoting 510 nm.¹²

Extended Systems

To further test the favorability oligomer formation, canonical ensemble (NVT) plane-wave DFT molecular dynamics simulations were performed with 10 Tc₂O₅ monomers at a liquid-like density of 1.6 g/mL, about half the density of Tc₂O₇(s). Plane-wave density functional theory (PW-DFT)^{17,18} canonical ensemble (NVT) molecular dynamics simulations were performed with the Vienna *ab initio* simulation package (VASP) version 5.4.1 using the PBE-D3^{2,3}. The projector augmented wave (PAW) pseudo-potentials formulated for PBE GW calculations were used to represent the ionic cores, and the valence configurations were 4s²4p⁶5s²5d⁵ for Tc and 2s²2p⁴ for O.¹⁹ The Γ -point alone was used to represents the first Brillouin zone. The plane waves were cut off at 600 eV. The energy convergence criterion for an SCF cycle is 10⁻⁶ eV. The molecular dynamics used a time step of 2 fs and ran for 10 ps. The simulation volume was a cube with a 12 Å side length, and 5 different initial guesses for the placement of 10 optimized bent corner sharing Tc₂O₅ molecules were used. The initial velocities were generated from a randomly generated Maxwell-Boltzmann distribution around the input temperature of 300 K, and the Nose-Hoover thermostat was used to control the temperature. Along the trajectories stacking and extended chain formation was observed, and edge-sharing Tc connections and bonding of a Tc to a neighboring molecule's bridging oxygen was also observed. Example snapshots taken from the trajectories exhibiting these oligomerization motifs may be seen in Figure S5. While the time scale, 10 ps, and simulation setup is insufficient to make any concrete conclusions, it does appear that a condensed Tc₂O₅ would have a very diverse, frequently muting self-reactivity which could easily explain why no solid, crystalline form of ‘tech red’ has ever been successfully isolated unlike Re₂O₅,^{20–23} which is still known to disproportionate into +4 and +7 species.²⁴

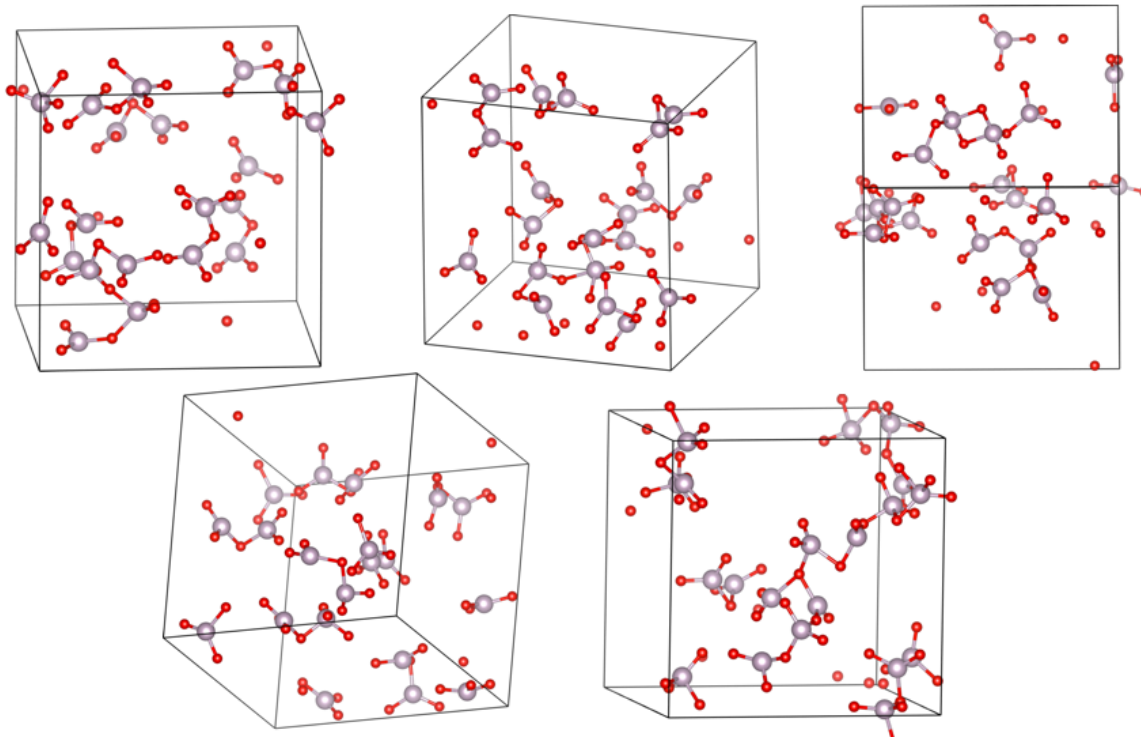


Figure S5: Snapshots taken from NVT-MD simulations of 10 1-br Tc_2O_5 molecules in a $(12 \text{ \AA})^3$ cube displaying several possibilities for self-reactivity of Tc_2O_5 molecules.

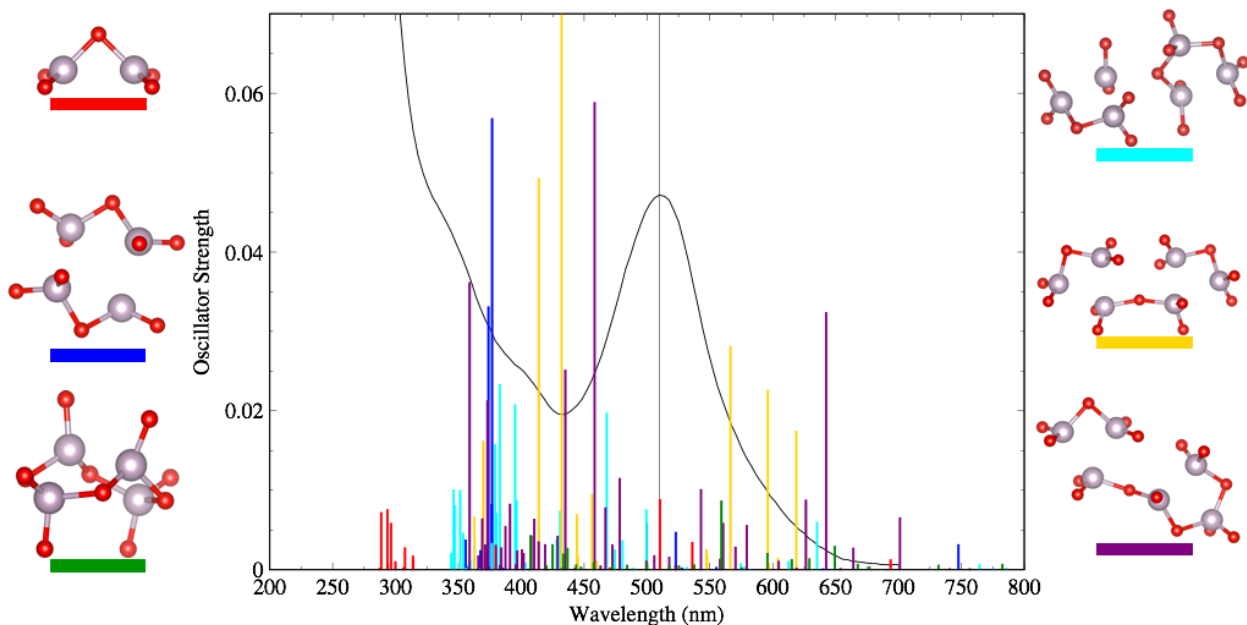


Figure S6: TD-DFT predicted UV-Vis absorption spectra for identified dimers and trimers of 1-br Tc_2O_5 . The experimental curve (scaled by $\frac{1}{4}$) for the red product is overlaid along with a thin line denoting 510 nm.¹²

Functional group additions away from basic oxides

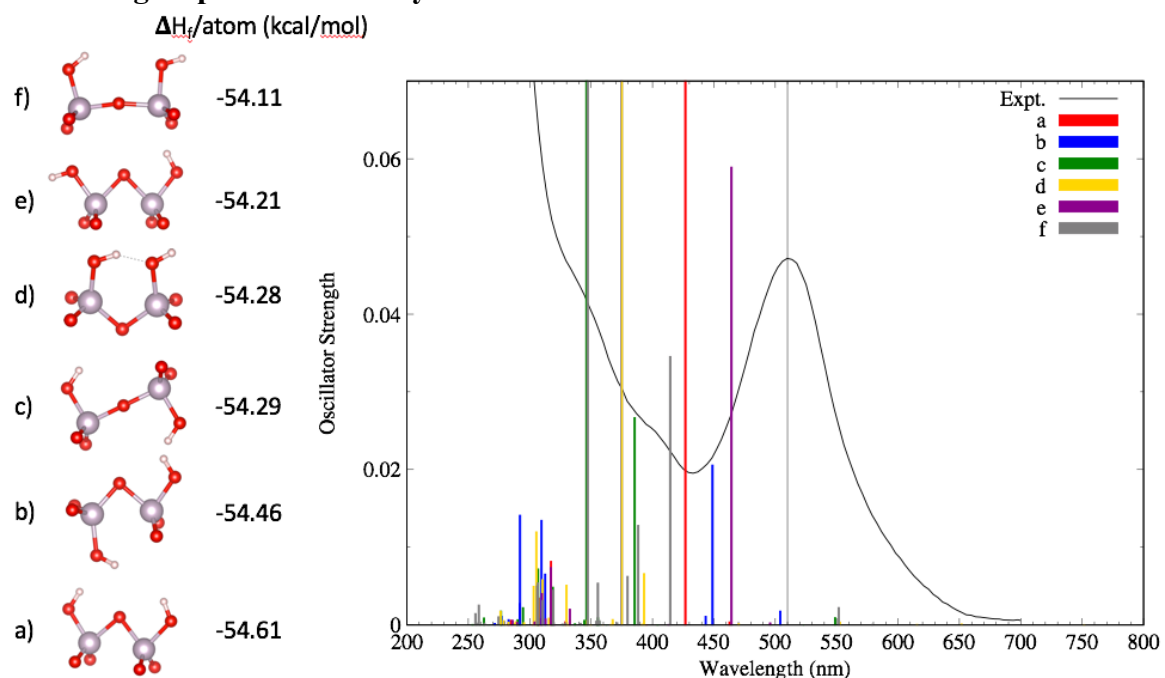


Figure S7: The structures, heat of formation per atom, and TD-DFT predicted UV-Vis spectra of the 6 lowest energy conformers of 1-br $\text{Tc}_2\text{O}_5 + 2\text{OH}$. The experimental curve (scaled by $\frac{1}{4}$) for the red product is overlaid along with a thin line denoting 510 nm.¹² All structures are singlets.

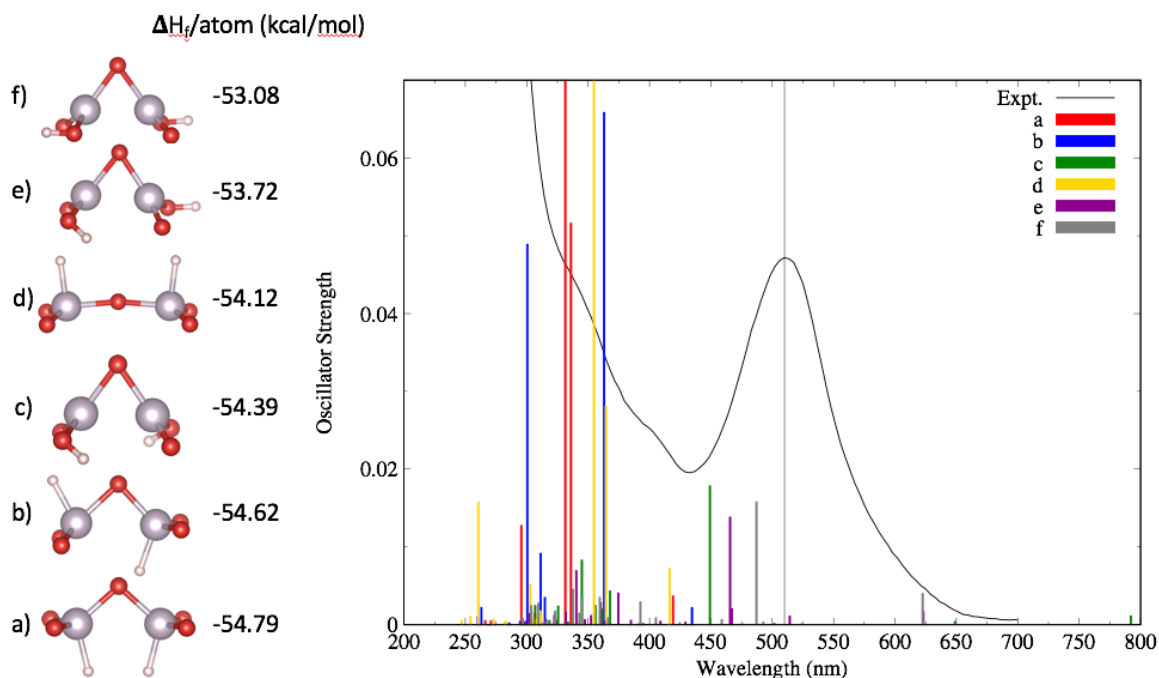


Figure S8: The structures, heat of formation per atom, and TD-DFT predicted UV-Vis spectra of the 6 lowest energy conformers of 1-br $\text{Tc}_2\text{O}_5 + 2\text{H}$. The experimental curve (scaled by $\frac{1}{4}$) for the red product is overlaid along with a thin line denoting 510 nm.¹² All structures are singlets.

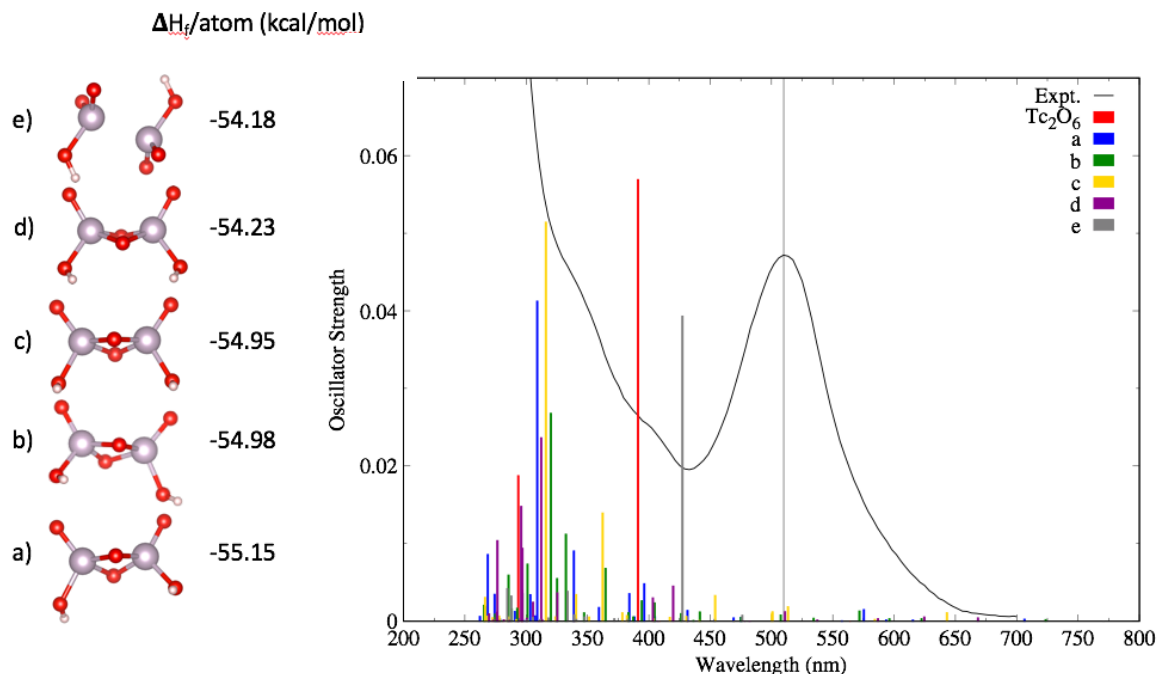


Figure S9: The structures, heat of formation per atom, and TD-DFT predicted UV-Vis spectra of the 5 lowest energy conformers of 2-br $\text{Tc}_2\text{O}_6 + 2\text{H}$. The experimental curve (scaled by $\frac{1}{4}$) for the red product is overlaid along with a thin line denoting 510 nm.¹² d) is a triplet, all the rest are singlets.

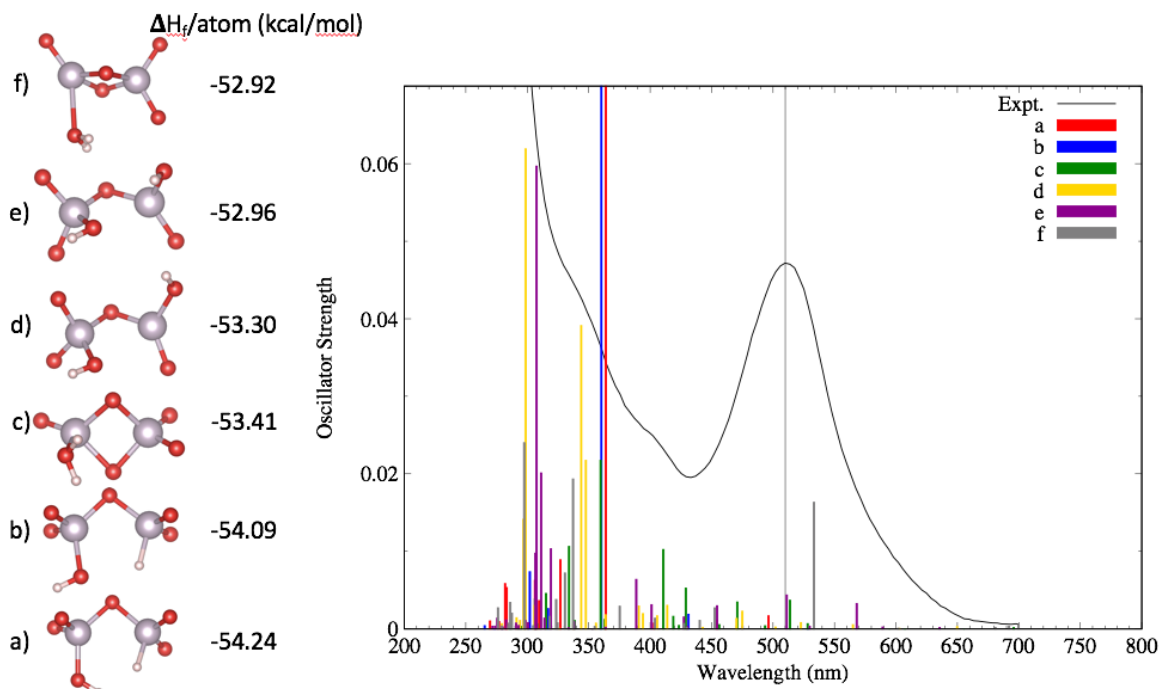


Figure S10: The structures, heat of formation per atom, and TD-DFT predicted UV-Vis spectra of the 6 lowest energy conformers of 1-br $\text{Tc}_2\text{O}_5 + \text{H}_2\text{O}$. The experimental curve (scaled by $\frac{1}{4}$) for the red product is overlaid along with a thin line denoting 510 nm.¹² e) and f) are triplets, all the rest are singlets.

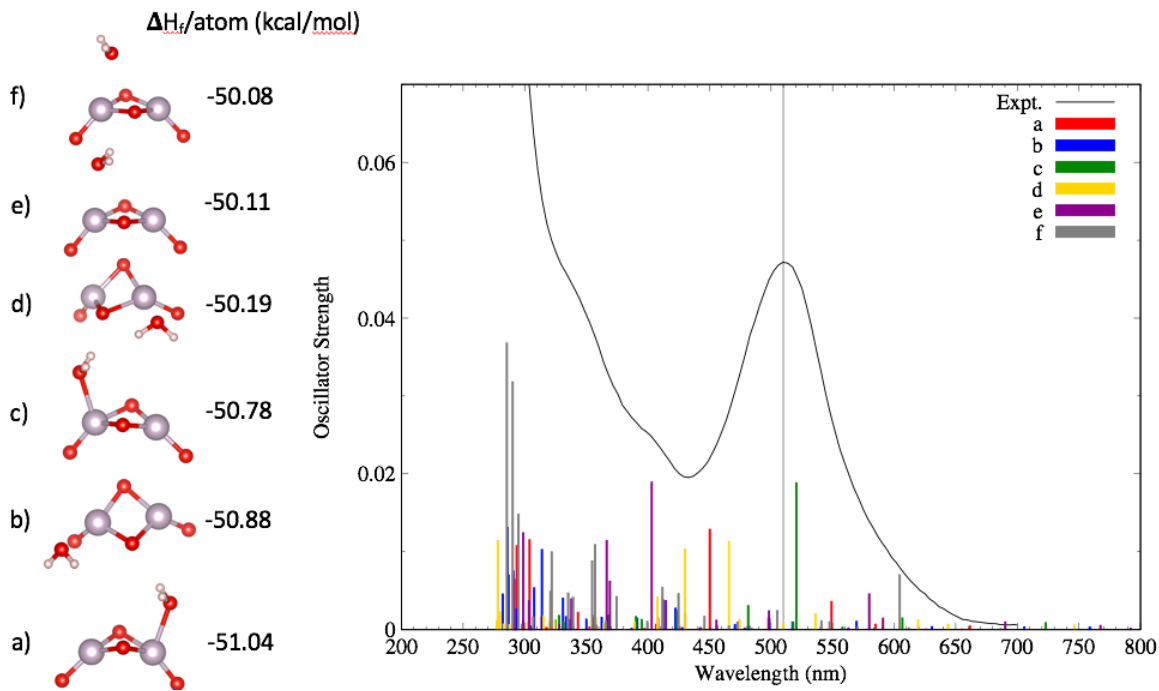


Figure S11: The structures, heat of formation per atom, and TD-DFT predicted UV-Vis spectra of the 6 lowest energy conformers of 2-br $\text{Tc}_2\text{O}_4 + \text{H}_2\text{O}$. The experimental curve (scaled by $1/4$) for the red product is overlaid along with a thin line denoting 510 nm.¹² d) is a quintet, a,e,f) are triplets, c,d) are singlets.

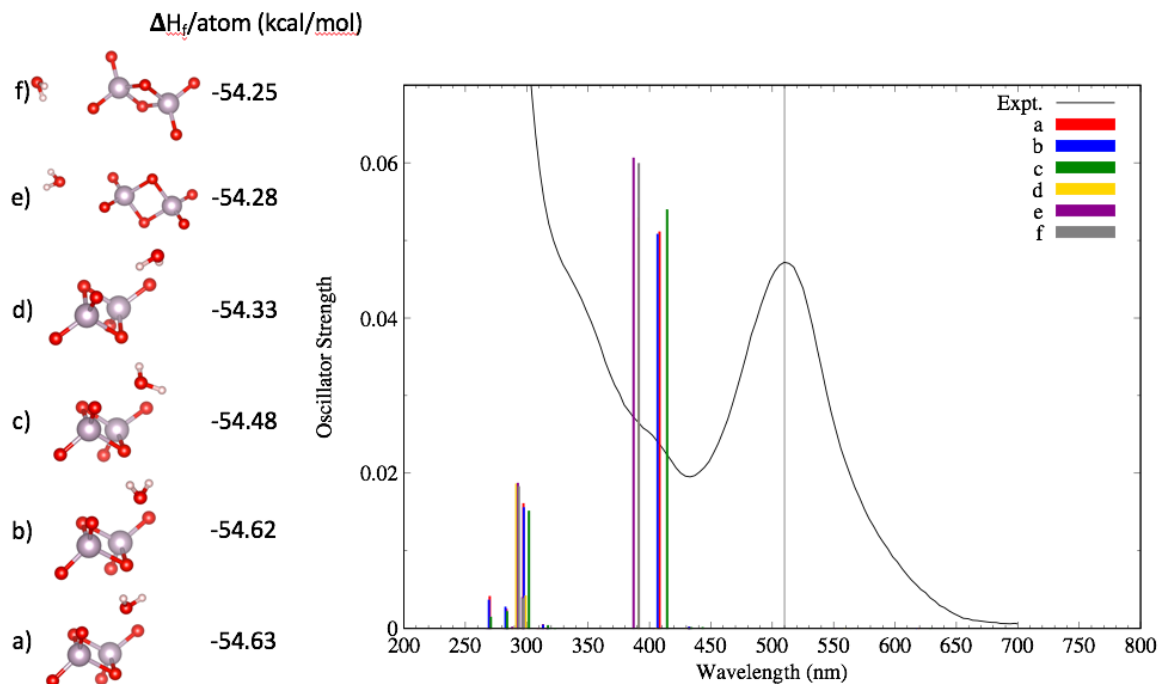


Figure S12: The structures, heat of formation per atom, and TD-DFT predicted UV-Vis spectra of the 6 lowest energy conformers of 2-br $\text{Tc}_2\text{O}_6 + \text{H}_2\text{O}$. The experimental curve (scaled by $1/4$) for the red product is overlaid along with a thin line denoting 510 nm.¹² All structures are singlets.

References

- (1) Shao, Y.; Gan, Z.; Epifanovsky, E.; Gilbert, A. T. B.; Wormit, M.; Kussmann, J.; Lange, A. W.; Behn, A.; Deng, J.; Feng, X.; Ghosh, D.; Goldey, M.; Horn, P. R.; Jacobson, L. D.; Kaliman, I.; Khaliullin, R. Z.; Ku, T.; Landau, A.; Liu, J.; Proynov, E. I.; Rhee, Y. M.; Richard, R. M.; Rohrdanz, M. A.; Steele, R. P.; Sundstrom, E. J.; Lee, H.; Iii, W.; Zimmerman, P. M.; Zuev, D.; Albrecht, B.; Alguire, E.; Austin, B.; Beran, G. J. O.; Bernard, Y. A.; Berquist, E.; Brandhorst, K.; Bravaya, K. B.; Brown, S. T.; Casanova, D.; Chang, C.-M.; Chen, Y.; Chien, S. H.; Closser, K. D.; Crittenden, D. L.; Diedenhofen, M.; Distasio, R. A.; Do, H.; Dutoi, A. D.; Edgar, R. G.; Fatehi, S.; Fusti-Molnar, L.; Ghysels, A.; Golubeva-Zadorozhnaya, A.; Gomes, J.; Hanson-Heine, M. W. D.; Harbach, P. H. P.; Hauser, A. W.; Hohenstein, E. G.; Holden, Z. C.; Jagau, T.-C.; Ji, H.; Kaduk, B.; Khistyayev, K.; Kim, J.; King, R. A.; Klunzinger, P.; Kosenkov, D.; Kowalczyk, T.; Krauter, C. M.; Lao, K. U.; Ele, A.; Laurent, D.; Lawler, K. V.; Levchenko, S. V; Lin, C. Y.; Liu, F.; Livshits, E.; Lochan, R. C.; Luenser, A.; Manohar, P.; Manzer, S. F.; Mao, S.-P.; Mardirossian, N.; Marenich, A. V.; Maurer, S. A.; Mayhall, N. J.; Neuscamman, E.; Oana, C. M.; Olivares-Amaya, R.; O 'neill, D. P.; Parkhill, J. A.; Perrine, T. M.; Peverati, R.; Prociuk, A.; Rehn, D. R.; Rosta, E.; Russ, N. J.; Sharada, S. M.; Sharma, S.; Small, D. W.; Sodt, A.; Stein, T.; Stück, D.; Su, Y.-C.; Thom, A. J. W.; Tsuchimochi, T.; Vanovschi, V.; Vogt, L.; Vydrov, O.; Wang, T.; Watson, M. A.; Wenzel, J.; White, A.; Williams, C. F.; Yang, J.; Yeganeh, S.; Yost, S. R.; You, Z.-Q.; Zhang, I. Y.; Zhang, X.; Zhao, Y.; Brooks, B. R.; Chan, G. K. L.; Chipman, D. M.; Cramer, C. J.; Goddard Iii Ah, W. A.; Gordon, M. S.; Hehre, W. J.; Klamt, A.; Schaefer Iii Aj, H. F.; Schmidt, M. W.; Sherrill, C. D.; Truhlar, D. G.; Warshel, A.; Xu, X.; Aspuru-Guzik, A.; Baer, R.; Bell, A. T.; Besley, N. A.; Chai, J.-D.; Dreuw, A.; Dunietz, B. D.; Furlani, T. R.; Gwaltney, S. R.; Hsu, C.-P.; Jung, Y.; Kong, J.; Lambrecht, D. S.; Liang, W.; Ochsenfeld, C.; Rassolov, V. A.; Slipchenko, L. V; Subotnik, J. E.; Voorhis, T. Van; Herbert, J. M.; Krylov, A. I.; Gill, P. M. W.; Head-Gordon, M. Advances in Molecular Quantum Chemistry Contained in the Q-Chem 4 Program Package. *Mol. Phys.* **2015**, *113*, 184–215.
- (2) Perdew, J. P.; Burke, K.; Ernzerhof, M. Generalized Gradient Approximation Made Simple. *Phys. Rev. Lett.* **1996**, *77*, 3865–3868.
- (3) Grimme, S.; Antony, J.; Ehrlich, S.; Krieg, H. A Consistent and Accurate Ab Initio Parametrization of Density Functional Dispersion Correction (DFT-D) for the 94 Elements H-Pu. *J. Chem. Phys.* **2010**, *132*, 1–19.
- (4) Andrae, D.; Häussermann, U.; Dolg, M.; Stoll, H.; Preuss, H. Energy-Adjustedab Initio Pseudopotentials for the Second and Third Row Transition Elements. *Theor. Chim. Acta* **1990**, *77*, 123–141.
- (5) Weigend, F.; Ahlrichs, R. Balanced Basis Sets of Split Valence, Triple Zeta Valence and Quadruple Zeta Valence Quality for H to Rn: Design and Assessment of Accuracy. *Phys. Chem. Chem. Phys.* **2005**, *7*, 3297.
- (6) Childs, B. C.; Braband, H.; Lawler, K.; Mast, D. S.; Bigler, L.; Stalder, U.; Forster, P. M.; Czerwinski, K. R.; Alberto, R.; Sattelberger, A. P.; Poineau, F. Ditechnetium Heptoxide Revisited: Solid-State, Gas-Phase, and Theoretical Studies. *Inorg. Chem.* **2016**, *55*, 10445–10452.
- (7) Lawler, K. V.; Childs, B. C.; Mast, D. S.; Czerwinski, K. R.; Sattelberger, A. P.; Poineau, F.; Forster, P. M. Molecular and Electronic Structures of M₂O₇ (M = Mn, Tc, Re). *Inorg. Chem.* **2017**, *56*, 2448–2458.

- (8) Rohrdanz, M. A.; Herbert, J. M. Simultaneous Benchmarking of Ground- and Excited-State Properties with Long-Range-Corrected Density Functional Theory. *J. Chem. Phys.* **2008**, *129*, 34107.
- (9) Peach, M. J. G.; Benfield, P.; Helgaker, T.; Tozer, D. J. Excitation Energies in Density Functional Theory: An Evaluation and a Diagnostic Test. *J. Chem. Phys.* **2008**, *128*, 44118.
- (10) Richard, R. M.; Herbert, J. M. Time-Dependent Density-Functional Description of the $^1\text{L}_a$ State in Polycyclic Aromatic Hydrocarbons: Charge-Transfer Character in Disguise? *J. Chem. Theory Comput.* **2011**, *7*, 1296–1306.
- (11) Vydrov, O. A.; Scuseria, G. E. Assessment of a Long-Range Corrected Hybrid Functional. *J. Chem. Phys.* **2006**, *125*, 234109.
- (12) Childs, B. C.; Lawler, K. V.; Braband, H.; Mast, D. S.; Bigler, L.; Stalder, U.; Peterson, D. R.; Jansen, A.; Forster, P. M.; Czerwinski, K. R.; Alberto, R.; Sattelberger, A. P.; Poineau, F. The Nature of the Technetium Species Formed during the Oxidation of Technetium Dioxide with Oxygen and Water. *Eur. J. Inorg. Chem.* **2017**, *Submitted*, 1–22.
- (13) Adamo, C.; Barone, V. Toward Reliable Density Functional Methods without Adjustable Parameters: The PBE0 Model. *J. Chem. Phys.* **1999**, *110*, 6158.
- (14) Becke, A. D. A New Mixing of Hartree–Fock and Local Density-Functional Theories. *J. Chem. Phys.* **1993**, *98*, 1372.
- (15) Yanai, T.; Tew, D. P.; Handy, N. C. A New Hybrid Exchange–correlation Functional Using the Coulomb-Attenuating Method (CAM-B3LYP). *Chem. Phys. Lett.* **2004**, *393*, 51–57.
- (16) Vlahović, F.; Perić, M.; Gruden-Pavlović, M.; Zlatar, M. Assessment of TD-DFT and LF-DFT for Study of D – D Transitions in First Row Transition Metal Hexaaqua Complexes. *J. Chem. Phys.* **2015**, *142*, 214111.
- (17) Hohenberg, P.; Kohn, W. Inhomogeneous Electron Gas. *Phys. Rev. B* **1964**, *136*, 864–871.
- (18) Kohn, W.; Sham, L. J. Self-Consistent Equations Including Exchange and Correlation Effects*. *Phys. Rev. A* **1965**, *140*, 1133–1138.
- (19) Lejaeghere, K.; Bihlmayer, G.; Bjorkman, T.; Blaha, P.; Blugel, S.; Blum, V.; Caliste, D.; Castelli, I. E.; Clark, S. J.; Dal Corso, A.; de Gironcoli, S.; Deutsch, T.; Dewhurst, J. K.; Di Marco, I.; Draxl, C.; Du ak, M.; Eriksson, O.; Flores-Livas, J. A.; Garrity, K. F.; Genovese, L.; Giannozzi, P.; Giantomassi, M.; Goedecker, S.; Gonze, X.; Granas, O.; Gross, E. K. U.; Gulans, A.; Gygi, F.; Hamann, D. R.; Hasnip, P. J.; Holzwarth, N. A. W.; Iu an, D.; Jochym, D. B.; Jollet, F.; Jones, D.; Kresse, G.; Koepernik, K.; Kucukbenli, E.; Kvashnin, Y. O.; Locht, I. L. M.; Lubeck, S.; Marsman, M.; Marzari, N.; Nitzsche, U.; Nordstrom, L.; Ozaki, T.; Paulatto, L.; Pickard, C. J.; Poelmans, W.; Probert, M. I. J.; Refson, K.; Richter, M.; Rignanese, G.-M.; Saha, S.; Scheffler, M.; Schlipf, M.; Schwarz, K.; Sharma, S.; Tavazza, F.; Thunstrom, P.; Tkatchenko, A.; Torrent, M.; Vanderbilt, D.; van Setten, M. J.; Van Speybroeck, V.; Wills, J. M.; Yates, J. R.; Zhang, G.-X.; Cottenier, S. Reproducibility in Density Functional Theory Calculations of Solids. *Science (80-)*. **2016**, *351*, aad3000-aad3000.
- (20) Nechamkin, H.; Hiskey, C. F.; Moeller, T.; Shoemaker, C. E. Rhenium(VI): Oxide (Rhenium Trioxide); John Wiley & Sons, Inc.; pp 186–188.
- (21) Tribalat, S.; Delafos, D.; Piolet, C. Sur Un Nouvel Oxyde de Rhénium: L’oxyde de Rhénium (V). *Comp. Rend.* **1965**, *261*, 1008–1011.
- (22) Borisova, L. V.; Ryabchikov, D. I.; Yarinova, T. I. Rhenium Compounds in Sulfuric Acid

- Solutions in the Presence of Reducing Agents. *Zh. Neorg. Khim.* **1968**, *13*, 321–328.
- (23) Colaïtis, D.; Lebas, D.; Lécaille, C. Un Oxyde de Rhenium En Relation de Structure Avec V₂O₅. *Mater. Res. Bull.* **1973**, *8*, 627–634.
- (24) Greenwood, N. N.; Earnshaw, A. *Chemistry of the Elements*, Second Ed.; Reed Educational and Professional Publishing Ltd: Oxford, 1997.